Polymers as Dewetting Agents

Régis Fondecave and Françoise Brochard Wyart*

Physico-Chimie Curie, Institut Curie and University Paris 6, 11 rue Pierre et Marie Curie, 75231 Paris Cedex 05

Received January 26, 1998; Revised Manuscript Received September 29, 1998

ABSTRACT: We study the stability of a film of poly(dimethylsiloxane) with an oligomer as the solvent. On a silanated Si−wafer, the solvent wets, but the polymer does not. We find that at all polymer volume fraction ϕ, films below a critical thickness $e_c(\phi)$ are unstable. We observe two regimes of dewetting vs ϕ: (i) classical "*dry" dewetting* for $\phi > \phi_L$, where the film ruptures in a multitude of droplets on a dry solid; (ii) unusual "*wet*" *dewetting* for $\phi < \phi_L$, where the final droplets coexist with a film of pure solvent. In this new regime, $e_c(\phi)$ is found to scale like $\phi^{0.80\pm0.01}$. We interpret these results via an equilibrium between droplets of solution and a solid covered by a film of pure solvent. This equilibrium occurs if $\phi < \phi_L$, the critical concentration. At $\phi = \phi_L$ we have a "leak out" transition of the solvent. All these results can be extended to other complex systems, where wetting processes and phase separation are coupled.

General Aims

The dewetting of *pure liquid films* forced onto nonwettable solid[1−3] or liquid[4,5] surfaces and exposed to air or onto a deformable solid (a rubber)[6] has been intensively studied in the recent past. A number of practical problems are controlled by these dewetting processes: fast drying induced by chemical agents, stability of coating films, hydroplaning of motor cars, stability of the lacrymal film with and without soft contact lenses, color printing, etc. Liquid films dewet below a critical thickness e_c, either by nucleation and growth of dry patches[1−6] or by spinodal decomposition:[7] holes nucleate spontaneously, and the film ruptures in a multitude of droplets, arranged in polygons.[8] The critical thickness for dewetting, e_c, is also the thickness of large sessile drops, flattened by gravity.[9]

However, in all practical applications, the formulation of a liquid implies a complex mixture of additives. Our aim here is to extend the laws of dewetting obtained with pure liquids to binary mixtures. We study a challenging case: a liquid mixture with antagonist components: the solvent wets (the spreading parameter $S_0 > 0$), but the solute does not ($S_1 < 0$).

In the *first section*, we describe the system and the respective wetting properties of the two components separately.

In the *second section*, we study the wetting laws for *microscopic* droplets of polymer solutions. We study the contact angle θ vs the polymer volume fraction ϕ. The spreading parameter $S(\phi)$ is positive for $\phi = 0$ and negative for $\phi = 1$. One could expect a wetting transition at ϕ_w , where $\theta(\phi_w) = 0$. Instead, we observe a plateau value $\theta = \theta_L$ below a critical concentration $\phi_L > \phi_w$. This corresponds to the "leak out transition" predicted first by Boudoussier[10] and observed by us very recently.[11] This transition results from a competition: the solvent likes the polymer, but it also likes the wettable substrate. For $\phi > \phi_L$, the droplet keeps its solvent, and is in contact with the dry solid. For $\phi < \phi_L$, attraction by the solid wins, the solvent escapes, and the droplet of solution is surrounded by a precursor film of pure solvent ("fried egg" configuration). The leak out transition masks the wetting transition, and the contact angle remains finite at all compositions.

In *the third part*, we study macroscopic droplets flattened by gravity because the thickness of these droplets defines the stability of films of solutions. Microscopic droplets behave like a microosmometer: the concentration inside the droplet is fixed by the equality of the solvent chemical potentiel in the drop and in the "halo". Macroscopic droplets behave like a "reservoir", and the volume fraction ϕ is fixed. We measure the contact angle θ vs ϕ, the thickness $e_c(\phi)$ of the large drops flattened by gravity, and the thickness e_ϕ of the film of pure solvent in equilibrium with the "reservoir" drop.

In *the fourth part*, we study the dewetting of films of polymer solutions for compositions above and below the leak out threshold ϕ_L.

$\phi > \phi_L$ is "dry" dewetting: the film ruptures in droplets, deposited on a *dry* solid.

$\phi < \phi_L$ is "wet" dewetting: the film ruptures in droplets, now deposited on a *wet* solid.

The System : Wedding of Partial and Complete Wetting

The wetting by a nonvolatile liquid of a smooth chemically homogeneous solid substrate is well understood.[12−19] The control parameter is the spreading coefficient S,[14] giving the energy difference between bare and wet substrate

$$S = \gamma_{SO} - (\gamma_{SL} + \gamma) \tag{1}$$

where the γ_{ij} are respectively the solid/air, solid/liquid, and liquid/air interfacial tensions.

The sign of S separates two regimes.

(A) If $S > 0$, we have *complete wetting*, where a liquid drop deposited onto the solid surface spreads completely and ultimately becomes a flat pancake, of thickness e_0.[15−19] e_0 results from a competition between long-range forces which tend to thicken the film and S, written as[15]

$$S = e\Pi + P \tag{2}$$

where $P(e)$ is the contribution of long-range van der Waals forces ($P(e) = A/12\pi e^2$, where A is the solid/liquid Hamaker constant assumed to be positive) and $\Pi(e) = -\,dP/de$ is the disjoining pressure.[13,20]

10.1021/ma980098q CCC: $15.00
Published on Web 12/04/1998

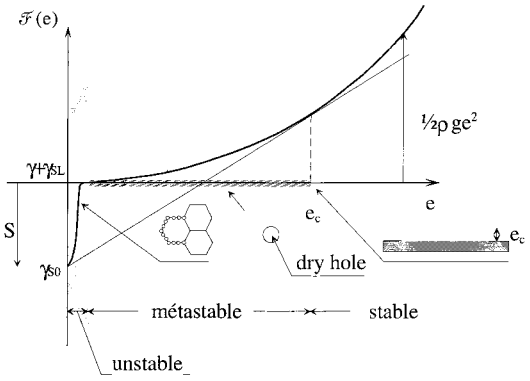

Figure 1. Free energy of a wet solid per unit area vs film thickness e. The Maxwell construction shows the coexistence between a film of thickness e_c and the dry solid, which corresponds to large sessile drops flattened by gravity. All films below e_c dewet (i) by nucleation and growth of a dry patch for thick film ($F''(e) > 0$) or (ii) by spinodal decomposition for thin films ($F''(e) < 0$).

Equation 2 gives a thickness $e_0 = a\sqrt{3\gamma/2S}$, where a is a nanoscopic length defined by $A/6\pi = \gamma a^2$.

(B) If $S < 0$, we have *partial wetting*, where a liquid drop remains localized on a small area. A small drop achieved a spherical cap, with a contact angle θ defined by the Young relation:

$$\gamma_{S0} = \gamma_{SL} + \gamma \cos \theta_E \tag{3}$$

A large drop is flattened by gravity. Its thickness e_c results from a balance between gravity forces and S, written as:[21]

$$-S = \frac{1}{2}\rho g e_c^2 \tag{4}$$

where ρ is the liquid density and g the acceleration gravity.

The stability of a liquid film, as shown in Figure 1, depends on the sign of S. If $S > 0$, case A, films are always stable. If $S < 0$, case B, films are unstable and dewet below a critical thickness e_c. e_c is also the thickness of large drops flattened by gravity, which corresponds to an equilibrium between the solid and a flat film. Thin films dewet spontaneously, while thicker films are metastable and dewet by nucleation and growth of a dry patch.

We have built a system where the pure solvent wets (regime A), and the solute does not wet (regime B).

The *substrate* is an oxidized silicon wafer, grafted with a monolayer of hexa- (HTS) or octadecyltrychlorosilanes (OTS), prepared by the method of Sagiv.[22,23] The critical surface tension, measured by using an alkane series, is $\gamma_c = 20.2 \pm 0.3$. The hysteris measured from the difference between advancing and receding contact angles is extremely low ($\theta_a - \theta_r \sim 2°$ for $\theta \sim 10°$).

The solvent is an oligomer "P dimethylsiloxane" of P monomers. We have studied three molecular weights, $M_w = 770$, 950, and 1250, corresponding to $P = 10$, 12, and 17. The characteristics are given in Table 1. γ has been measured by the Wilhelmy method. For these three oligomers, $\gamma < \gamma_c$, and they wet the substrate. We show in Figure 2a the profile of a spreading microdroplet. The final stage is a "pancake" of thickness 10 Å for $P = 10$. The thickness e_0 increases with P, as shown in Table 1.

The polymer is a N dimethylsiloxane ($M_w = 91\,700$), with $N = 1230$ or larger. The surface tension of the polymer is larger than γ_c . A small droplet achieved a spherical cap, with a contact angle $\theta = 20.4°$ (Figure 2b). From θ, one can deduce the value of the polymer spreading coefficient $S_1 = -1.30 \pm 0.02$ mN m^{-1}. The critical thickness below which a film dewets, deduced from eq 4, is 520 μm.

The solvent wets, and the polymer dewets: what happens if we mix these two components? To answer this question, we have first to remember the fate of sessile microdroplets and the leak out transition of the solvent at ϕ_L . Then, to understand the stability of liquid films, we have to study the conformation of large drops, because their thickness is the critical thickness below which a film becomes unstable.

Sessile Microdroplets of Solutions: the Leak Out Transition[10,11]

Microdroplets (volume $\Omega \sim$nL) are gently deposited on the silanated silicon wafer with glass microcapillaries. The contact angles are measured optically by two methods.

(1) Reflection of a Laser Beam. The droplet acts like a convex mirror for a parallel light beam from a He−Ne laser, incident perpendicularly to the solid substrate. The divergence of the reflected beam is proportional to the contact angle θ at the contact line. This method[24] has an accuracy of ±0.5° and is used for $\theta > 4°$.

(2) Interferential Reflection Contrast Microscopy (RCIM). We show in Figure 3 the image of a droplet of solution observed with a microscope. From the interference fringes, one can construct the complete profile of the drop and extract the contact angle and the volume. This technic allows to measure with high accuracy (±0.01) small contact angles $1 < \theta < 4°$.

The pure solvent has a positive spreading coefficient S_0

$$S_0 = \gamma_{S0} - (\gamma_{SL0} - \gamma_0) \tag{5}$$

where γ_{SL0} and γ_0 are the solvent/solid and solvent/air interfacial tensions.

Table 1. Summary of Experimental Results[a]

M_w	P	N	γ (mN.m^{-1})	e_0 (Å)	$\theta°$ (deg)	ϕ_L	ϕ_w	a_p (Å)	x_e	a_c (μm)	x_c
770	10		19.2 ± 0.2	10 ± 1		0.54	0.47	6.5 ± 0.1	0.80 ± 0.01	204 ± 5	0.81 ± 0.12
950	12		19.3 ± 0.2	12 ± 1		0.47	0.41	6.6 ± 0.1	0.80 ± 0.01	201 ± 6	0.86 ± 0.13
250	17		19.6 ± 0.2	23 ± 1		0.29	0.26	9.0 ± 0.4	0.80 ± 0.02		
2000	27		20 ± 0.2		7°						
91700		1239	20.7 ± 0.2		20.4						

[a] Glossary: γ, surface tension; e_0, thickness of the wetting film of a pure solvent "van der Waals pancake". e_ϕ, thickness of the wetting film in equilibrium with a reservoir drop; $\theta°$, equilibrium contact angle; ϕ_L, volume fraction of the leak out transition; ϕ_W, volume fraction of the wetting transition; a_p, molecular characteristic length of van der Waals pancakes; x_e, exponent of the scaling law for e_ϕ; e_c, thickness of gravity pancakes; a_c, characteristic length of gravity pancakes; x_c, exponent of the scaling law for gravity pancakes.

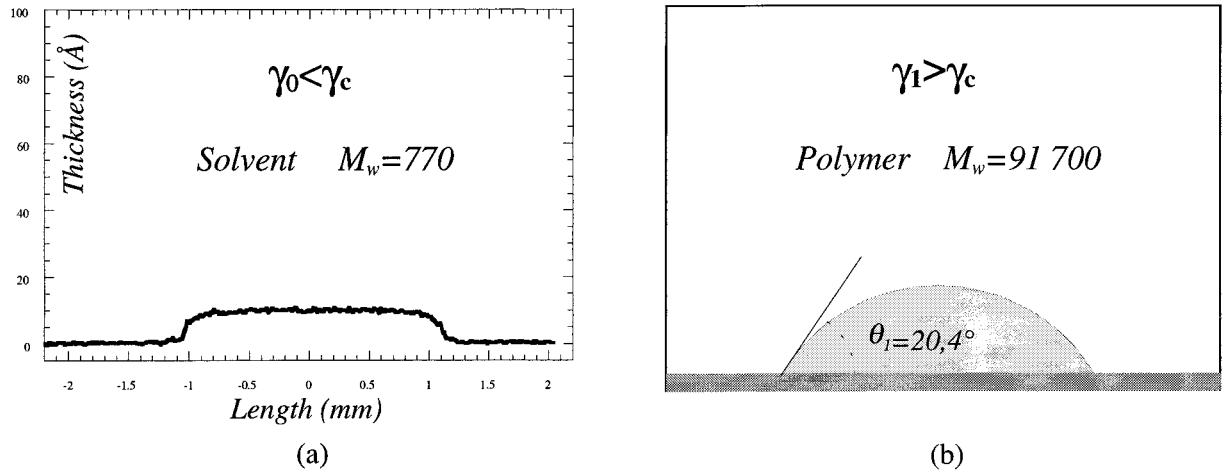

Figure 2. Wetting of the two components. (a) *Complete wetting of the pure solvent* ($M_w = 770$). The spreading of a sessile micro drop is monitored by ellipsometry. The final state is the "van der Waals pancake" of thickness e_o ($e_o = 10$ Å). (b) *Partial wetting of the polymer*. A droplet of pure polymer achieves at equilibrium a spherical cap, with a contact angle θ_1.

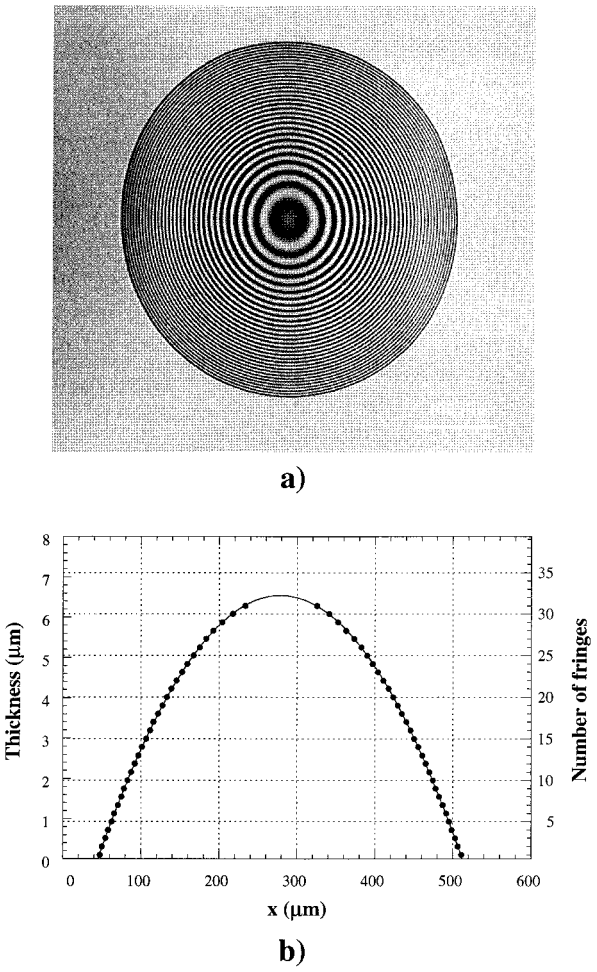

Figure 3. Image of a polymer droplet obtained by interference microscopy. From the interference fringes (a), one can construct the profile of the drop (b).

Adding polymer, we form a solution of polymer volume fraction ϕ. The spreading parameter $S(\phi)$ is positive for $\phi = 0$, and negative for $\phi = 1$. For intermediate ϕ values, we can write

$$S(\phi) = \gamma_{S0} - [(\gamma_{SL}(\phi) + \gamma(\phi)] = S(0) - \Delta\gamma(\phi) \quad (6)$$

The polymer is depleted at both interfaces: (a) at the liquid/air interface because $\gamma_1 > \gamma_0$; (b) at the passive solid/liquid interface, because small chains are entropically favored.[25] The polymer is in the semidilute regime, and can be pictured as a transient network of mesh size ξ.[26,27]

In a monomeric solvent, $\xi = a_0\phi^{-3/4}$, where a_0 is a monomer size. In an oligomer as a solvent, the excluded volume interactions are progressively screened as P increases. ξ becomes[28]

$$\xi = a_0 P^{1/4}\phi^{-3/4} \quad (7)$$

The osmotic pressure of the polymer solution $\Pi_{OSM}(\phi)$ scales like[29]

$$\Pi_{OSM} = \frac{kT}{\xi^3} \quad (8)$$

and is reduced as P increases.

The increase in surface tension $\Delta\gamma$ at both interface is the work required to expel the polymer from the depletion layer of thickness ξ.[17] We then have[30−32]

$$\Delta\gamma \sim \frac{kT}{\xi^2} \quad (9)$$

Clearly, the contact angle θ (ϕ) should decrease when the polymer concentration decreases. From the Young equation, $\theta(\phi)$ and $S(\phi)$ are related by

$$\sin^2\frac{\theta}{2}(\phi) = -\frac{S(\phi)}{2\gamma(\phi)} \quad (10)$$

Normally, we would expect a wetting transition[13] $\theta(\phi_w) = 0$ at a volume fraction ϕ_w such as $S(\phi_w) = 0$. The plot of $\theta(\phi)$ is different and is shown in Figure 4.

We observe two domains, separated by a critical composition ϕ_L (listed for various oligomers in Table 1): Above ϕ_L, the contact angle increases monotonically up to θ_L. Below ϕ_L the contact angle remains constant and equal to θ_L. Using an ellipsometer, we observe (Figure 5) that the droplet is surrounded by an halo, a nanoscopic film of thickness e_0, equal to the thickness of the van der Waals pancake of the pure solvent. We call it the "fried egg" drop. By extrapolation of the curve $\theta(\phi)$, one can determinate ϕ_w, but we do not reach a wetting transition at ϕ_w.

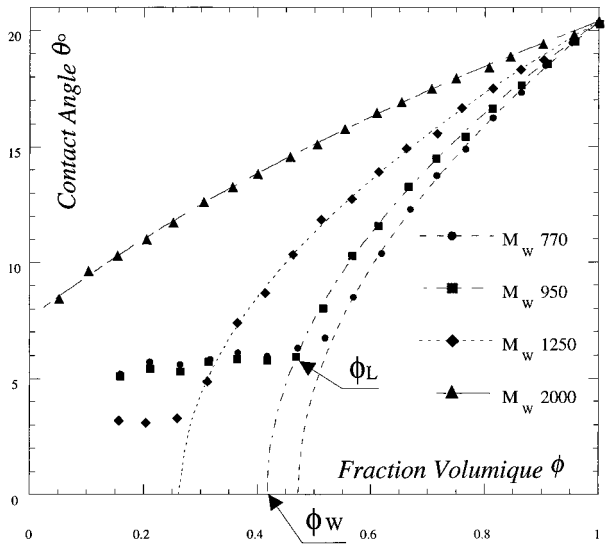

Figure 4. Contact angle of droplet of solution vs polymer volume fraction. $\theta(\phi)$ decreases up to a plateau value θ_L for $\phi < \phi_L$. ϕ_L and ϕ_w are the composition of the "leak out" and wetting (masked) transition respectively. The configuration of a droplet below ϕ_L is shown in Figure 6.

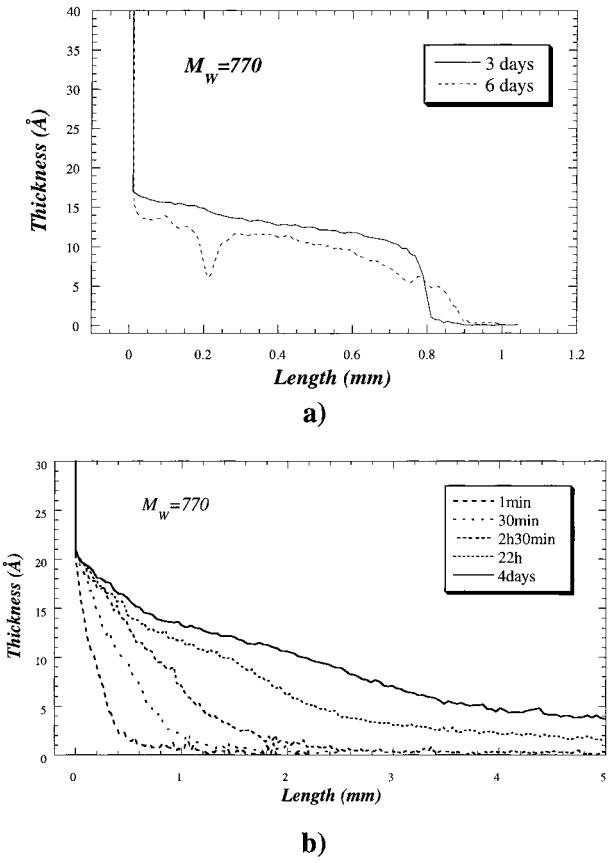

Figure 5. Ellipsometric profile of a precursor film emanating from the drop when $\phi < \phi_L$: (a) on HTS wafer at 3 and 6 days after the deposition (notice a sharp edge at thickness e_o and a degradation of the film at 6 days); (b) on OTS wafer, where the profiles are spread and characteristic of a 2d evaporation of the solvent molecule on the solid substrate.

We conclude that at and below ϕ_L, the solvent escapes from the droplet. It is why we named this new transition the "leak out transition".[11] Below ϕ_L, the "fried egg" droplet represented schematically in Figure 6 behaves like a microosmometer: the polymer in semidilute

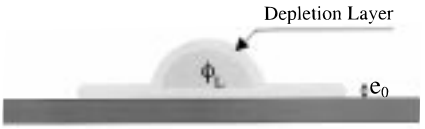

Figure 6. "Fried egg" configuration of a drop of polymer solution for $\phi < \phi_L$. The final state of a seesile droplet is a spherical cap of polymer solution at fixed composition ϕ_L, surrounded by a halo of pure solvent. At equilibrium, the osmotic pressure in the drop balances the disjoining pressure in the film.

solution in the drop is excluded from the surrounding film because $e_0 < \xi_L$, the correlation length at $\phi = \phi_L$. The drop/film equilibrium is ruled by the equality of the solvent chemical potentiel in the two phases $\mu_{S,drop} = \mu_{S,film}$, written as

$$\frac{kT}{\xi_L^3} = \frac{\gamma a^2}{e^3} \tag{11}$$

The halo of solvent coexists with the solid. This imposes $S = e\pi + P$; i.e., $e = e_0$.

Then

$$\xi_L = e_0 \left(\frac{kT6\pi}{A}\right)^{1/3} \tag{12}$$

Remark 1: To observe this equilibrium, the volume Ω of the droplet has to be very small ($\Omega \sim 100$ to 10^{-1} nL for dilute droplets), such that the substrate is not entirely covered by the precursor film.

Remark 2: the wetting transition is masked because $\phi_w < \phi_L$. The only control parameter is $\tilde{A} = A/kT$ as shown in ref 10, and $\phi_L = \phi_W$ defines a critical value $\tilde{A}_c$. For $\tilde{A} > \tilde{A}_c$, $\phi_w > \phi_L$ and the wetting transition will be observable. All regimes in the phase diagram $\tilde{A}$, ϕ are discussed in ref 33.

Conclusion. We find two regimes for the spreading of a droplet. Above ϕ_L we observe a spherical cap, with a composition ϕ in polymer. Below ϕ_L we have been able to observe "fried egg" droplets, where a spherical cap containing the solution at composition ϕ_L is surrounded by an halo of pure solvent, as shown in Figure 6.

These experiments on the wetting of small droplets of solutions, which may seem very simple, are in fact extremely difficult. We have been faced with three problems:

(1) 3d Evaporation. Even if the solvents are not volatile, a degradation of the van der Waals "pancake" is observed after 1 or 2 days. The values of the contact angle (Figure 4) correspond to measurements made when the precursor film starts to degradate. However, these values are very closed to the contact angles measured at ϕ_L, showing that the system has nearly reached its equilibrium state.

(2) 2d Evaporation. The film which emanates from the drop (Figure 5a) has a sharp border of thickness e_0. In some other cases, Figure 5b, the profiles are spread, and characteristic of a 2d evaporation. The solvent does not achieve a condensed liquid pancake, but a 2d gas phase on the solid substrate. This explains why the most delicate part of this study is the silanization of the wafer. In the first experiment,[11] silanization was performed with OTS ($\gamma_c = 20.4$). Despite the extremely weak hysteresis, the oligomer $P = 10$ on these substrate presents the 2d evaporation shown in Figure 5b. Then we changed the silane and used HTS (hexadecyltrichlo-

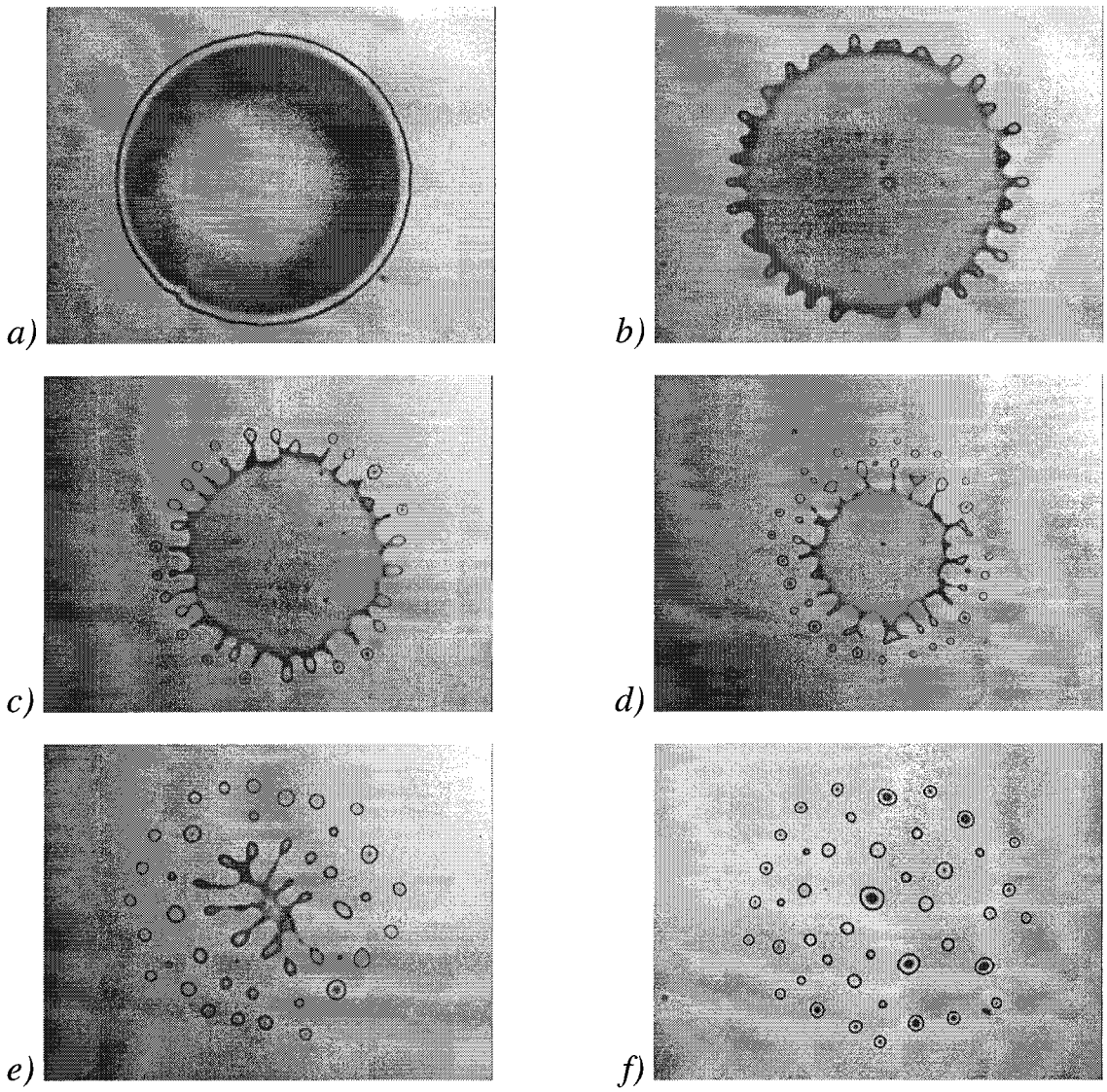

Figure 7. Marangoni instability of dilute drop of polymer solution ($\phi = 0.005$; $M_w = 770$). (1) The drop spread too much and too fast. The shape becomes flat. (2) Undulation of the contour is observed coupled to the formation of an unstable rim and digitation, whereas the contact line receeds (dewetting). (3) The figure breaks into droplet and a rim is reformed, which contracts toward the center. (4, 5) Interactions of the process are observed. (6) Final stage: microdroplets are left on the substrate.

cosilane). On this "HTS" wafer, the 2d evaporation is no longer observed. One has however to be careful, because the aging of these surfaces induced by repeted washing (sonication + ultrason + chloroform) may lead to a degradation of the molecular carpet and a 2d evaporation (after about 10 washes) even on HTS wafers.

(3) Marangoni Instabilities. When we deposite droplets of volume fraction ϕ less than 0.15, a Marangoni instability of the droplet contour is observed (Figure 7). This instability has been widely studied.[34−38] Its origin is due to a gradient of surface tension, which results either from a thermal gradient for volatile liquids[34−37] or from a concentration gradient[38] for binary mixtures. In our case, as the solvent escapes, the polymer concentration increases at the wedge of the drop and induces a gradient of surface tension. As observed for volatile droplets,[37] the dynamics of spreading accelerates ($R(t) \sim t^{1/3}$ instead of $t^{1/10}$) and the drops profile becomes flat and surrounded by a rim, which breaks into droplets, while it receeds. The final state are microdroplets dispersed on the substrate, which are too small to be observed by interferometry.

An amazing image of two unstable drops close together (Figure 8) shows the presence of the microscopic film, which emanates from the drops.

Reservoir "Drops" (Φ = cte)

We have studied in the preceding section the configuration of microscopic droplets, which expulse the solvent and adjust their initial volume fraction ϕ ($\phi < \phi_L$) to the value ϕ_L to realize the three phases solid/film/drop equilibrium.

We will study now the opposite case of large millimetric drops, of volume fraction ϕ, not modified by the formation of the film of solvent. The drop plays the role of an infinite reservoir of solvent. If we let the solvent film grow, all of the substrate will become wet. The final thickness of the film, now called e_ϕ, is given by the balance between disjoining and osmotic pressures:

$$\Pi_{vw}(e_\phi) = \Pi_{osm}(\phi) \qquad (13)$$

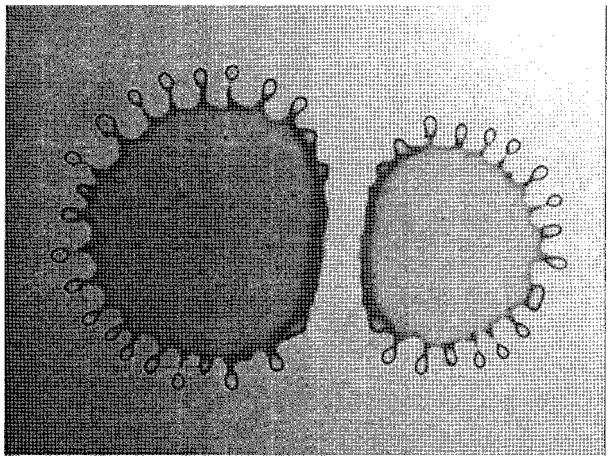

Figure 8. Digitation of two neighboring droplets. One can see on this image the presence of the precursor film: when the two solvent films meet the Marangoni instability is neutralized.

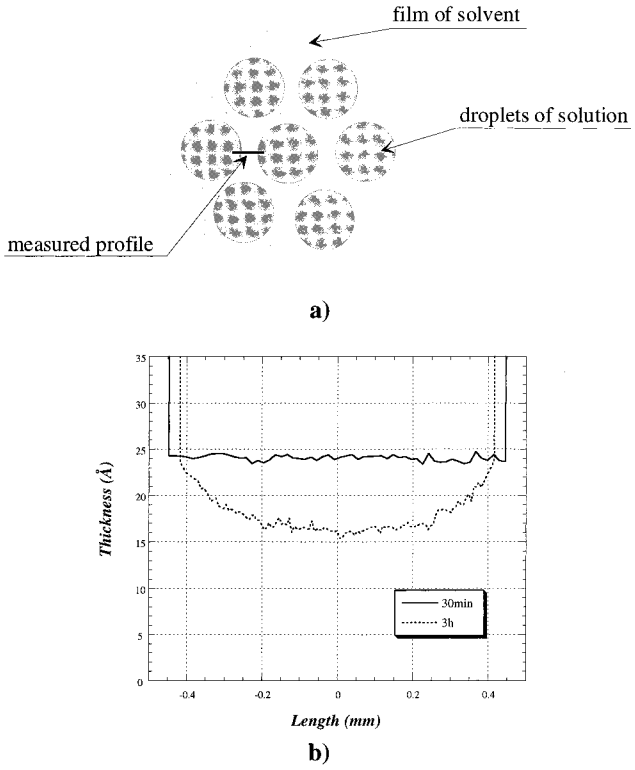

Figure 9. (a) Reservoir drops (composition ϕ) and coexisting wetting film. (b) Ellipsometric profile of the film between two drops: (A) before equilibrium (t = 30 mn); (B) after equilibrium (t = 3 h), where the thickness e_ϕ is uniform.

This equality leads to

$$\frac{A}{6\pi e_\phi^{\,3}} = \frac{kT}{\xi^3} \tag{14}$$

Inserting in eq 15 the expression for ξ (eq 7) leads to

$$e_\phi = a_0 \tilde{A}^{1/3} P^{1/4} \Phi^{-3/4} \tag{15}$$

To determine e_ϕ we have deposited several droplets of volume fraction ϕ (Figure 9a), and we measured by ellipsometry the nanoscopic film in equilibrium with the drops (Figure 9b). Another method is to monitor one single drop and to measure the thickness profile $e_\phi(x)$

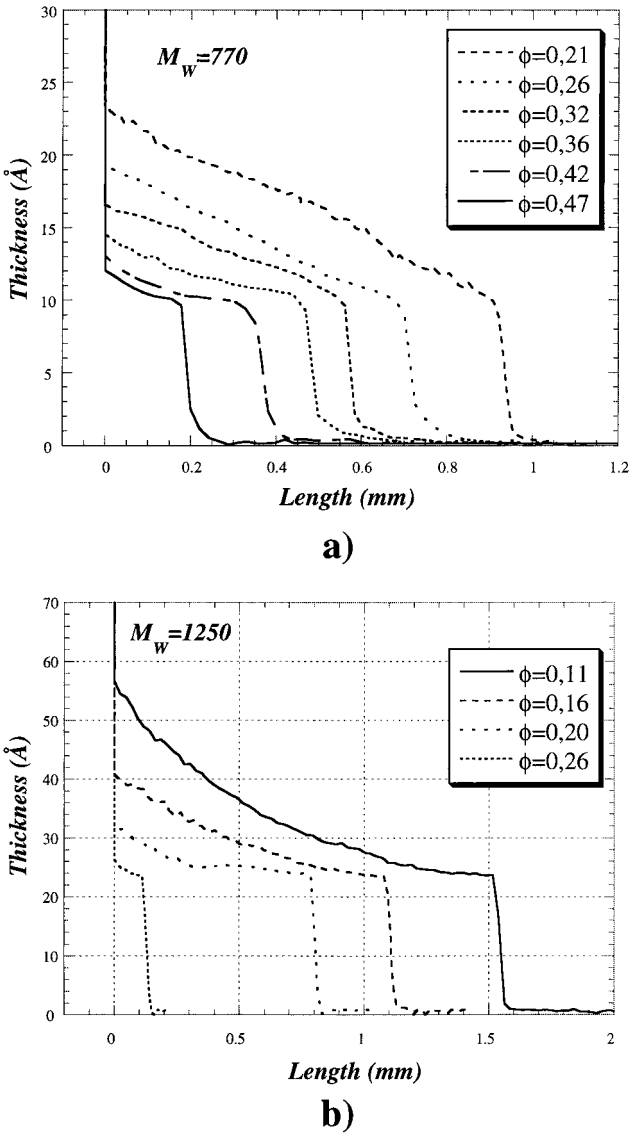

Figure 10. Ellipsometric profile of the precursor film for various polymer volume fraction f for two solvents: (a) M_w = 770; (b) M_w = 1250. e_ϕ is the thickness at the drop/film line, and e_o is that at the film/solid edge.

of the solvent film emitted from the drop (Figure 10). The thickness at the border of the drop (x = 0) is the equilibrium thickness e_ϕ as checked by comparing the values obtained by the two methods. The resulting plot of e_ϕ vs ϕ is shown in Figure 11 in logarithmic coordinates for three oligomers. e_ϕ follows the power law

$$e_\phi = a_p \phi^{-x_e}, \quad x_e = 0.80 \pm 0.02 \tag{16}$$

where a_p is a microscopic length (which varies from 6.5 Å for P = 10 to 9 Å for P = 17). Values of a_p and x_e are listed in Table 1.

The exponent 0.8 is close to the value 0.75 expected for a semidilute polymer solution in a good solvent (eq 15). The prefactor increases with P, which indicates a screening of the monomer interaction by the P chains according to eq 15.

Conclusion. The study of reservoir droplets has demonstrated two fundamental results.

(1) The thickness of the precursor film at the droplet's border is directly related to the volume fraction of the drop. We have built an osmometer. We have used this

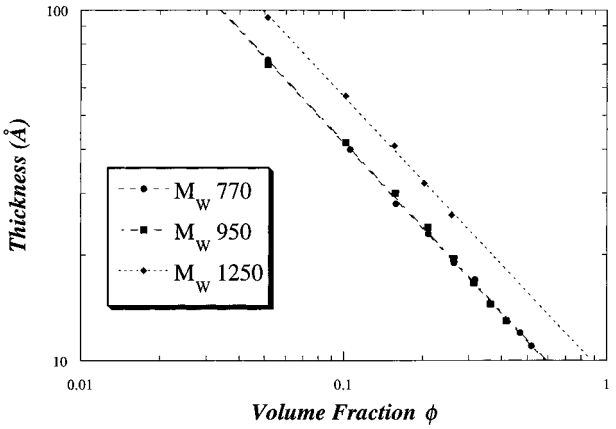

Figure 11. Thickness e_ϕ of solvent film vs polymer volume fraction ϕ in logarithmic scales, for three oligomers.

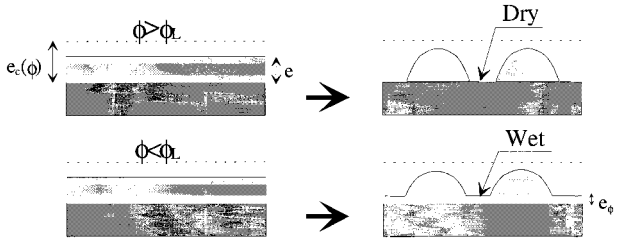

Figure 12. The two regimes of dewetting: $\phi > \phi_L$, "dry" dewetting; $\phi < \phi_L$, "wet" dewetting.

conclusion to derive the volume fraction vs time in the "leaking" microscopic droplets, by a measure of the thickness of the film at the contact line between the drop and the wet solid. For a droplet of solution (oligomer $P = 10$), we start with a volume fraction $\phi_i = 0$, 2 and $e_\phi = 24$ Å. After 6 days, $e_\phi = 14$ Å. From Figure 11, we conclude that the volume fraction has increased to the value $\phi = 0.4$.

(2) The increase of the thickness e_ϕ with dilution is well fitted by the power law $e_\phi \sim \phi^{0.80\pm0.02}$, close to the theoretical value (0.75) predicted for a polymer in a good solvent.

Dewetting of Polymer Solutions

The dewetting of pure polymer PDMS films had been studied first by C. Redon.[1] A film dewets below a critical thickness

$$e_c(1) = 2\kappa^{-1} \sin\frac{\theta_1}{2}$$

e_c is the thickness of the large drops flattened by gravity. Thick films are metastable: one must nucleate a dry patch, which grows if its radius R is larger than R_c, the critical nucleation radius, comparable to the initial film thickness e. Microscopic films ($e < \pi m$) are unstable, and break spontaneously into a multitude of droplets arranged in polygons:[7] one names this regime "spinodal decomposition" by analogy with phase transitions.

We will next show here the dewetting of polymer solution in the two regimes shown schematically in Figure 12.

$\Phi > \Phi_L$: Dry Dewetting (Figure 12a). When $\Phi > \Phi_L$, the solution droplets are in condition of classical "partial wetting", i.e., deposited on a dry solid. These solutions behave like simple liquids, with a contact angle $\theta(\phi)$. $e_c(\phi)$ can be deduced from $\theta(\phi)$ by the classical relationship $e_c(\phi) = 2\kappa^{-1} \sin(\theta/2)(\phi)$. We show in Figure 13a the final state after the rupture of a thin PDMS film ($e \sim \pi m$): droplets are arranged in polygons.

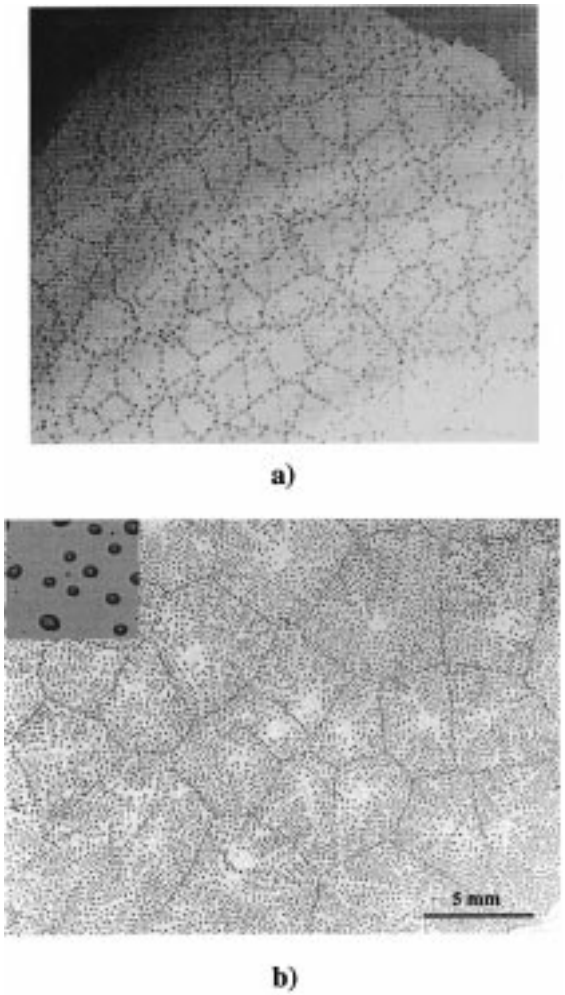

Figure 13. Final stage of the film after a spontaneous dewetting. (a) "Dry" dewetting. The multitude of droplets are arranged in polygons on a dry solid. (b) "Wet" dewetting ($\phi = 0.42$, $M_w = 770$). The polygons are now full of droplets, uniform in size, deposited on a *wet* solid. The thickness e_ϕ of the film between the droplets is 14 Å.

$\Phi < \Phi_L$: Wet Dewetting (Figure 12b). The particularity of this situation is that after the film's rupture, the substrate is covered by a nanoscopic film of thickness $e_c(\phi)$ in coexistence with droplets of polymer solution.

We show in Figure 13b a typical picture of spontaneous dewetting. One sees a multitude of droplets arranged in polygons, but the polygons are now full of droplets. Between the droplets, we have confirmed the existence of a film of thickness e_ϕ by ellipsometry.

In the case of the dewetting of pure PDMS, shown for comparison in Figure 13a, the droplets are arranged in polygons, which are empty. When holes are formed at random, they grow and are surrounded by a rim. When the rims of adjacent holes meet, they break into droplets, which form the polygons.

In the case of dewetting of mixtures, the moving rims exhibit a fingering instability and break itself into droplets, grow again, and break again, before adjacent rims meet to form the polygons. The net result of this cascade of Rayleigh instability and fingering are droplets, which are relatively monodisperse in size. The

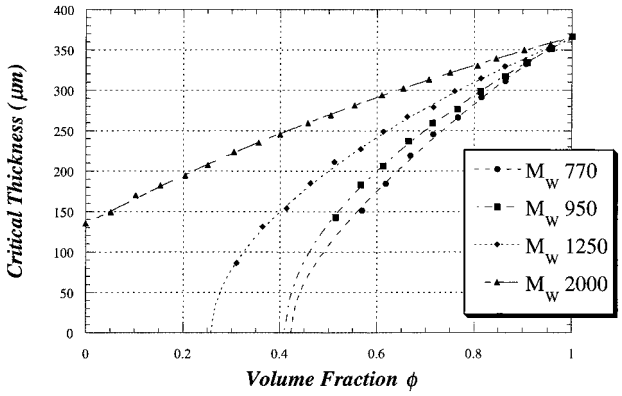

Figure 14. Critical thickness $e_c(\phi)$ for *dry* dewetting.

origin of this difference between "dry" and "wet" dewetting must be due to a Marangoni effect, also observed in the spreading of drops (Figure 7).

We study now the critical thickness $e_c(\phi)$ below which films are unstable, for the two situations of dry/wet dewetting. Film are expected to dewet at all compositions, but $e_c(\phi)$ has to tend to zero with ϕ, because films of pure solvent are stable, whatever their thickness: ($e_c(0) = 0$).

(A) Critical Thickness $e_c(\phi)$ for "Dry" Dewetting. For $\Phi > \Phi_L$, the solution behaves like a simple liquid, and $e_c(\phi)$ is given by

$$e_c = \sqrt{\frac{-2S}{\rho g}} \tag{17}$$

But here the spreading parameter S and the density ρ are composition dependent:

$$S(\phi) = \gamma_{S0} - \gamma(\phi) - \gamma_{SL}(\phi)$$

$$\rho(\phi) = \phi\rho_p + (1 - \phi)\rho_s$$

where ρ_p and ρ_s are *the mass per unit volume of* the polymer and the solvent, respectively.

Equation 17 can also be written in term of the contact angle $\theta(\phi)$

$$e_c(\phi) = 2\kappa^{-1} \sin\frac{\theta(\phi)}{2}$$

with

$$\kappa^{-1} = \sqrt{\frac{\gamma(\phi)}{\rho(\phi)g}} \tag{18}$$

In our case, $\kappa^{-1}(\phi)$ is rather constant ($\kappa^{-1}(1) = 1.47$ mm, $\kappa^{-1}(0) = 1.46$ mm for oligomer $P = 10$) and all the variation is contained in $\theta(\phi)$. Using for $\theta(\phi)$ the values measured with the small droplets (Figure 4) at composition $\Phi > \Phi_L$ we have plotted in Figure 14 the critical thickness $e_c(\phi)$ for four oligomers.

(B) Critical Thickness $e_c(\phi)$ for "Wet" Dewetting. I. Theoretical Predictions. In this case, droplets after dewetting are surrounded by a film of pure solvent. The film's thickness e_ϕ discussed previously results from a balance between disjoining and osmotic pressure:

$$\Pi_{osm}(\phi) = \Pi_{vw}(e_\phi) \tag{19}$$

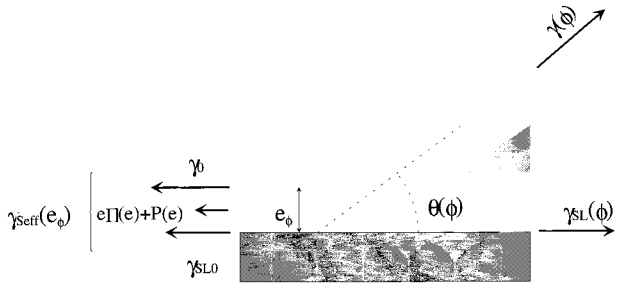

Figure 15. Forces acting on (a) a liquid wedge and (b) a gravity drop deposited on a *wet* solid.

The droplets are not in equilibrium with the dry solid, and the classical Young relation cannot apply. We have to define an effective surface energy of the wet solid $\tilde{\gamma}_{SO}$.

The free energy of the solid (surface Σ) covered by a film of thickness e is

$$F(e) = [\gamma_{SLO} + \gamma_O + P(e)]\Sigma$$

$$F(o) = \gamma_{SO}\Sigma \tag{20}$$

where γ_o and γ_{SLO} are the solvent/air and solvent/solid interfacial tensions, $P(e)$ is the long-range van der Waals contribution, which shows up for thin films ($P(\infty) = 0$, $P(0) = S_0$), and γ_{SO} is the bare solid surface energy.

From eq 20, one can derive the effective surface energy of the wet solid

$$\tilde{\gamma}_{S0} = \frac{\partial F(e)}{\partial \Sigma}\Big]_{\Omega=\Sigma e} \tag{21}$$

We deduce

$$\tilde{\gamma}_{so}(e) = \gamma_o + \gamma_{SLo} + (e\Pi + P)$$

$$\tilde{\gamma}_{So}(o) = \gamma_{S0} \tag{22}$$

We can also, in the same way, define an effective spreading parameter $\tilde{S}$, which will depend on composition and film thickness

$$\tilde{S} = \tilde{\gamma}_{SO}(e_\phi) - \gamma(\phi) - \gamma_{SL}(\phi) \tag{23}$$

where e_ϕ is the thickness of the film in equilibrium with the drop.

For the drop exposed to the wet solid, we can now write an extended Young equation which results from a balance between capillary forces and disjoining pressure (Figure 15)

$$\tilde{\gamma}_{So} = \gamma(\phi)\cos\theta(\phi) + \gamma_{SL}(\phi) \tag{24}$$

The critical thickness $e_c(\phi)$ for dewetting is the thickness of the large drop flattened by gravity. The balance of capillary, gravity and long-range forces in the film lead to the classical law, with $\tilde{S}$ instead of S

$$\frac{1}{2}\rho g e_c^2(\phi) = -\tilde{S} \tag{25}$$

From eqs 23−25, one finds the classical relation

$$e_c(\phi) = 2\kappa^{-1} \sin\frac{\theta(\phi)}{2} \tag{26}$$

We can calculate $\theta(\phi)$ and $e_c(\phi)$ for semidilute polymer solution; assuming that polymer is depleted at both interfaces, we can write

$$\gamma_{SL}(\phi) + \gamma(\phi) = \gamma_{SL}(o) + \gamma_o + \Delta\gamma(\phi) \qquad (27)$$

where

$$\Delta\gamma(\phi) = \frac{kT}{\xi^2}$$

$\xi = aP^{1/4}\Phi^{-3/4}$ is the correlation length.

The expression for $\tilde{S}(\phi)$ becomes

$$\tilde{S}(\phi) = (e\pi + P)_{e_\phi} - \Delta\gamma(\phi) \qquad (28)$$

Inserting in $\tilde{S}(\phi)$ the coexistence film/drop relation

$$\left(\pi(e_\phi) = \pi_{osm} = \frac{kT}{\xi^3}\right)$$

we get

$$\tilde{S}(\phi) = p\frac{kT}{\xi^2} \qquad (29)$$

where p is a constant, which depends only upon A/kT.

In the limit of small angle θ (ϕ), $\tilde{S} \approx {}^1/_2\gamma\theta^2(\phi)$.

Equations 24 and 25 lead to

$$\theta(\phi) \approx \frac{a}{\xi} \approx \phi^{3/4}$$

$$e_c(\phi) \approx \kappa^{-1}\frac{a}{\xi} \approx \phi^{3/4} \qquad (30)$$

Experimental Determination of $e_c(\phi)$

The principle used to derive $e_c(\phi)$ is to prepare a film of thickness $e < e_c(\phi)$. The film dewets, and when the droplets in coexistence with the film equilibrate, we can measure the contact angle of the drops $\theta(\phi)$ by interferometry. The critical thickness is deduced from $e_c(\phi)$ by the relation

$$e_c(\phi) = 2\kappa^{-1}\sin\frac{\theta}{2}(\phi) \cong \kappa^{-1}\theta(\phi) \qquad (31)$$

Films of uniform thickness are prepared by spin coating a droplet of solution. Thin films (thicknesses in the micrometer range or less) dewet spontaneously, by nucleation of holes at defects. We have not studied systematically the dynamics of dewetting. But we observed that, as for the classical case studied by Redon, holes open at a constant velocity. The velocity is proportionnal to $V^* = \gamma/\eta(\phi)$, where $\eta(\phi)$ is the solution viscosity, and varies from 1 to 100 μm s^{-1}. At the end of the dewetting process, we measure the thickness e_ϕ of the film by ellipsometry, and the contact angle $\theta(\phi)$ by RCIM interferometry (reflection contrast interference microscopy).

The values obtained are shown in Figure 16. We plot in gray color the contact angle $\theta(\phi)$ measured for microdroplets and reservoir droplets. In black, the values obtained after dewetting. One can notice that the values of $\theta(\phi)$ obtained by dewetting coincide to the values measured with reservoir drops.

We have also plotted in Figure 17 the critical thickness $e_c(\phi)$ proportional to $\theta(\phi)$, eq 30, in a log−log plot.

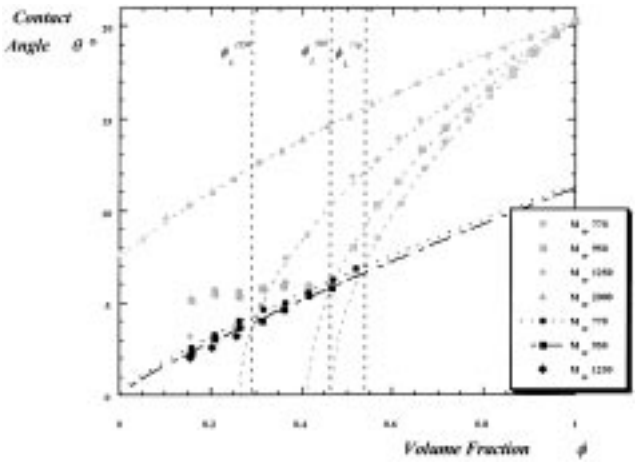

Figure 16. Contact angle $\theta(\phi)$ of droplets formed after the dewetting of a dilute film ($\phi < \phi_L$).

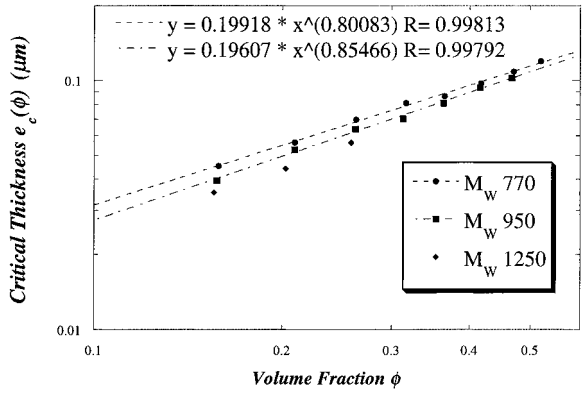

Figure 17. Critical thickness $e_c(\phi)$ for "wet" dewetting.

We conclude that $e_c(\phi)$ (and $\theta(\phi)$) can be adjusted by a power law

$$e_c(\phi) = a_c\phi^{x_c}$$

The values of a_c and x_c are listed in Table 1 for two oligomers.

The exponent $x_c \cong 0.8 \pm 0.1$ is in agreement with the theoretical exponent (0.75) expected for semidilute polymer solutions in good solvent conditions. The comparison of eq 16 giving film thickness e_θ (exponent 0.80 $\pm$ 0.01) and eq 32 show that the accuracy in measurements of e_θ is better than that for e_c. This is due to the fact that the precursor equilibrates very fast with the droplet. On the other hand, in the dewetting process, the final equilibrium is reached only after hours or days.

Concluding Remarks

We have studied the wetting and the dewetting of a binary mixture, with the following properties: (i) *antagonist wetting* properties are observed, where the solvent wets totally the substrate but the polymer does not; (ii) the polymer is under *good solvent* conditions; (iii) the polymer is *depleted* at both solid/liquid interfaces.

This system presents two remarkable features.

Phase Separation. The spreading induces a *phase separation* of two miscible liquids. We name this transition the "leak out" transition. The solvent is attracted by both the polymer and the solid substrate. At high concentration ($\phi > \phi_L$), the polymer wins and keeps its solvent. Below ϕ_L, the attraction by the solid dominates

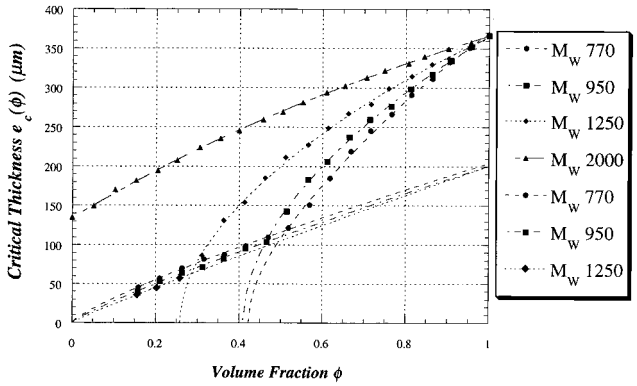

Figure 18. Critical thickness $e_c(\phi)$ for dewetting. One sees clearly a discontinuity of the slope of $e_c(\phi)$ at ϕ_L, corresponding to the crossover between dry (($\phi > \phi_L$) and wet ($\phi < \phi_L$) dewetting.

and the solvent escapes from the droplet and forms a precursor film. The long polymer chains are excluded from the nanoscopic film of solvent, because the confinement energy is huge.

Spreading droplets achieve "microosmometers". The droplet/film equilibrium imposes that the solvent chemical potential is uniform. This corresponds to the equality of the van der Waals *disjoining pressure* in the film, and the *osmotic pressure* in the droplet.

For *microdroplets*, which are so small that the precursor film does not cover the entire solid substrate, we have a three-phase coexistence: dry solid/wet solid (covered by a solvent film)/solution droplet. The dry/wet solid coexistence imposes the disjoining pressure and therefore the thickness ($e = e_0$) of the film. This fixes the droplet concentration to $\phi = \phi_L(\pi_{osm}(\phi_L) = \pi_{vw}(e_0)$. For macrodroplets, called reservoirs, the solid is completely wet. The drop composition (ϕ) is fixed. The equality of osmotic/van der Waals pressure imposes now the thickness e_ϕ of the film of solvent. Measurements by ellipsometry of e_ϕ allows to check the droplet composition, like in an osmometer.

Dewetting at All Polymer Concentrations. The film of pure solvent is stable, because the solvent wets totally the substrate. On the other hand, film of polymer solution are always unstable below a critical thickness $e_c(\phi)$.

We observe two regimes: (1) *dry wetting* ($\phi > \phi_L$), where after dewetting, the solid is bare, covered by droplets of solution; (2) *wet dewetting* ($\phi < \phi_L$), where droplets coexist with a film of pure solvent and $e_c(\phi)$ decreases to zero with a power law $e_c(\phi) \sim \phi^{0.80}$.

All these features observed here with PDMS polymers in solution in its oligomers can be extended to other systems, if the solute is depleted at both interface and if the thickness ξ of the depletion layer is larger than the thickness of the wetting film of pure solvent.

Large depletion thickness are observed with the polymer. One can recall other systems. (i) The first is *charged solutions*. Ions are repulsed at the water/air interface, and the thickness of the depletion layer is the Debye length κ_e^{-1}, which becomes large at weak ionic strengths. Experiments with polyelectrolytes are underway. Because in these systems, the osmotic pressure is very high, we expect a leak out transition at very low volume fraction. The difficulty of these experiments is to keep a substrate wettable to water, because high energy substrate are easily polluted. (ii) The second is *colloïdal suspensions*. Nanoparticules or emulsions are stabilized by ionic or steric repulsion. In the case of repulsive interfaces, the depletion layer is comparable to the particule size and is large, compared to the wetting film thickness. Similar behaviors are expected in this case.

(iii) The third is *binary mixtures* near the critical point. Compatible mixtures of small AB molecules with antagonist wetting properties may also phase separate if the concentration correlation length ξ becomes larger than the thickness of the wettable component.

We can even think of systems where both species wet the substrate, but the mixture does not! This may be the case for the same PDMS pair (long/small chains) deposited on a glycerol/water substrate.

This paper has established a few basic static properties: the existence of a critical thickness for dewetting (at all finite polymer volume fraction), the shape of reservoir drops, etc. The dynamic features are equally interesting: the early stages of dewetting by polymer solutions are, at the moment, unknown. We hope to study these features soon.

Acknowledgment. We thank Rhône Poulenc for its financial support and G. Schorsch, J. Daniel, and L. Vovelle for stimulating this work. We have benefited from many discussions with Axel Buguin, Georges Debregeas, and Pascal Martin at Institut Curie and Marie-Pierre Valignat, Anne-Marie Cazabat, and P. G. de Gennes at the College de France. We also thank Paul Chaikin for a rereading of the manuscript.

References and Notes

(1) Redon, C.; Brochard-Wyart, F.; Rondelez, F. *Phys. Rev. Lett.* **1991**, *66*, 715.
(2) Andrieu, C.; Sykes, C.; Brochard-Wyart, F. *J. Adhes.* **1996**, *58*, 15.
(3) Padday, J. F. S. *Spec. Discuss. Faraday Soc.* **1971**, *1*, 64. Sykes, C.; Andrieu, C.; Détappe, W. V.; Deniau, S.; Debregeas, G.; Brochard-Wyart, F. *J. Colloid Interface Sci.* **1997**, *190*, 134−141.
(4) Brochard-Wyart, F.; Martin, P.; Redon, C. *C. R. Acad. Sci. II* **1993**, *317*, 1539.
(5) Martin, P.; Buguin, A.; Brochard-Wyart, F. *Europhysics Lett.* **1994**, *28*, 421. Debregeas, G.; Martin, P.; Brochard-Wyart, F. *Phys. Rev. Lett.* **1995**, *75*, 3886. Faldi, A.; Composto, R. J.; Winey, K. *Langmuir* **1995**, *11*, 4855.
(6) Brochard-Wyart, F.; de Gennes, P. G. *J. Phys. Condens. Matter* **1994**, *6*, 9. Carré, A.; Shanahau, M. E. R. *Langmuir* **1995**, 3572.
(7) Brochard-Wyart, F.; Daillant, J. *Can. J. Phys.* **1990**, *68*, 409.
(8) Reiter, G. *Phys. Rev. Lett.* **1992**, *68*, 75. Reiter, G.; Schultz, J.; Auroy, P.; Auvray, L. *Europhys. Lett.* **1996**, *33*, 29. Zhao, W.; Rafailovich, M. M.; Sokolov, J.; Fetters, L. J.; Sauer, B. B. *Phys. Rev. Lett.* **1993**, *70*, 1453.
(9) Brochard-Wyart, F.; Redon, C.; Rondelez, F. *C. R. Acad. Sci.* **1988**, *306*, 1143.
(10) Boudoussier, M. *J. Phys. Paris* **1987**, *48*, 445.
(11) Fondecave, R.; Brochard-Wyart, F. *Europhysics Lett.* **1997**, *37*, 115.
(12) Brochard-Wyart, F.; di Meglio, J. M.; Quéré, M.; de Gennes, P. G. *Langmuir* **1991**, *7*, 335.
(13) de Gennes, P. G. *Rev. Mod. Phys.* **1985**, *57*, 827.
(14) Cooper, W.; Nuttal, W. *J. Agric. Sci.* **1915**, *7*, 219.
(15) Joanny, J. F.; de Gennes, P. G. *C. R. Acad. Sci.* **1984**, *299*, 279.
(16) Heslot, F.; Cazabat, A. M.; Levinson, P. *Phys. Rev. Lett.* **1989**, *62*, 1286.
(17) Daillant, J.; Benattar, J.; Bosio, L.; Léger, L. *Europhys. Lett.* **1988**, *6*, 431.
(18) Silberzan, P.; Léger, L. *Phys. Rev. Lett.* **1991**, *66*, 185.
(19) Valignat, M. P.; Fraysse, N.; Cazabat, A. M. *Langmuir* **1993**, *9*, 3255.
(20) Derjagin, B. *J. Phys. Chim. URSS* **1940**, *14*, 137.
(21) Bouasse, H. *Capillarité et Phénomènes Superficiels*; Delagrase: Paris, 1924.

(22) J. Sagiv *J. Am. Chem. Soc.* **1980**, *102*, 92.
(23) Brzoska, J. B.; Shahizadeh, N.; Rondelez, F. *Nature* **1992**, *360*, 24.
(24) Allain, C.; Ausserré, D.; Rondelez, F. *J. Colloid Interface Sci.* **1985**, *107*, 5.
(25) Semenov, A. N. Private communication.
(26) de Gennes, P. G. *Scaling Concepts in Polymer Physics;* Cornell University Press: Ithaca, NY, 1979.
(27) Daoud, M.; et al. *Macromolecules* **1975**, *8*, 804.
(28) Joanny, J. F.; Grant, P.; Turkevich, L. A.; Pincus, P. *J. Phys.* **1981**, *42*, 1045.
(29) des Cloizeaux, J. *J. Phys. (Paris)* **1975**, *36*, 281.
(30) Joanny, J. F.; Leibler, L.; de Gennes, P. G. *J. Polym. Sci. (Phys.)* **1979**, *17*, 1073.
(31) de Gennes, P. G. *Macromolecules* **1980**, *72*, 4756.
(32) de Gennes, P. G. *Macromolecules* **1981**, *14* , 1637.
(33) Fondecave, R. Ph.D. Thesis, University P. et M. Curie, Paris, Sept 1997.
(34) Huppert, H. E. *Nature* **1982**, *300*, 427.
(35) Troian, S. M.; Merbolzheimer, E.; Safran, S. A.; Joanny, J. F. *Europhys. Lett.* **1989**, *10*, 25.
(36) Brzoska, J. B.; Brochard-Wyart, F.; Rondelez, F. *Europhys. Lett.* **1992**, *19*, 97.
(37) Redon, C.; Brochard-Wyart, F.; Rondelez, F. *J. Phys II Fr.* **1992**, *2*, 1671.
(38) Fournier, J. B.; Cazabat, A. M. *Europhys. Lett.* **1992**, *20*, 512.

MA980098Q